

# Chloride Channel Activity of Bestrophin Mutants Associated with Mild or Late-Onset Macular Degeneration

Kuai Yu, Zhiqiang Qu, Yuanyuan Cui, and H. Criss Hartzell

**PURPOSE.** Mutations in the *hBest1* (*VMD2*) gene are linked to various kinds of macular degeneration, including Best vitelliform macular dystrophy (BVMD) and adult-onset vitelliform macular dystrophy (AVMD). The age at onset and severity of disease are quite variable. This study was conducted to examine  $\text{Cl}^-$  currents generated by six *hBest1* mutations (E119Q, A146K, T216I,  $\Delta$ I295, D312N, and L567F) found in patients having adult-onset macular dystrophies or in BVMD patients having normal electro-oculograms (EOGs), to examine the hypothesis that the severity of disease is related to the effect of the *hBest1* mutation on hBest1  $\text{Cl}^-$  channel function.

**METHODS.** Wild-type (WT) hBest1 was mutated by PCR-based mutagenesis. WT and mutant channels were expressed in HEK293 cells and  $\text{Cl}^-$  currents analyzed by whole-cell patch clamp. The trafficking of proteins to the plasma membrane was tested by cell-surface biotinylation.

**RESULTS.** All the mutations except L567F and T216I produced a defect in  $\text{Cl}^-$  channel function. The D312N and  $\Delta$ I295 mutants do not generate functional  $\text{Cl}^-$  currents. Furthermore, they inhibit WT hBest1 function. The amplitudes of currents produced by the A146K mutant were smaller than WT and had altered anionic selectivity. The E119Q mutant produced currents similar in amplitude to those of WT, but had altered relative permeability to large anions.

**CONCLUSIONS.** These findings support the idea that *hBest1* mutations produce variable forms of macular dystrophy via dysfunction of hBest1  $\text{Cl}^-$  channels. However, because the light peak of the EOG of some patients with the  $\Delta$ I295, D312N, E119Q, and A243V mutations does not correlate with the  $\text{Cl}^-$  channel function, the results also support the suggestion that the light peak of the EOG may not be generated solely by hBest1. (*Invest Ophthalmol Vis Sci.* 2007;48:4694–4705) DOI: 10.1167/iovs.07-0301

Mutations in human bestrophin-1 (*hBest1* or *VMD2*) are associated with Best vitelliform macular dystrophy (BVMD, OMIM 153700; Online Mendelian Inheritance in Man; <http://www.ncbi.nlm.nih.gov/Omim/>) provided in the public domain by the National Center for Biotechnology Information,

Bethesda, MD),<sup>1,2</sup> adult-onset vitelliform macular dystrophy (AVMD, OMIM 608161),<sup>3,4</sup> and autosomal recessive vitelliform vitreoretinopathy (ADVIRC OMIM 193220).<sup>5</sup> BVMD is classically described as an autosomal dominant, juvenile-onset disease. Large vitelliform deposits of a yellow-pigmented material accumulate in subretinal and sub-RPE spaces.<sup>6,7</sup> The lesion passes through a pseudohypopyon stage and is often accompanied by detachment of the neural retina from the RPE<sup>7–11</sup> before the deposits become disorganized (the vitelloruptive stage), the affected area degenerates, and loss of vision occurs. AVMD has similar vitelliform lesions but develops later in life.

A characteristic feature of BVMD is an abnormal light peak (LP) of the electro-oculogram (EOG).<sup>12–15</sup> The normal EOG voltage reaches a minimum (dark trough) during dark adaptation and increases slowly (~10 minutes) to a peak when the light is switched on (light peak). An Arden ratio, which is the amplitude of the *light peak* to the *dark trough*,<sup>12</sup> below 1.5 is generally considered pathologic. It is thought that the LP is generated by a  $\text{Cl}^-$  ion channel in the basolateral membrane of the RPE.<sup>16–18</sup> It has been proposed that light stimulates release of an “LP substance” (possibly adenosine triphosphate [ATP]) from the neural retina which acts on receptors on the RPE, elevates cytosolic  $\text{Ca}^{2+}$ , and activates a basolateral  $\text{Cl}^-$  conductance.<sup>17,19</sup>

Because bestrophins function as  $\text{Ca}^{2+}$ -regulated  $\text{Cl}^-$  channels<sup>20–27</sup> and Best1 is in the basolateral membrane of the RPE, it has been proposed that hBest1 is the  $\text{Cl}^-$  channel that generates the LP. All the disease-causing *hBest1* mutations that have been examined (T6P, A10V, Y85H, R92C, W93C, N99K, D104E, R218S, G222E, Y227N, A243T, A243V, Q293K, Q293H, G299E, E300D, D301E, and T307I) exhibit depressed  $\text{Cl}^-$  channel function.<sup>20,28,29</sup> Many of these mutations also inhibit wild-type (WT) currents during coexpression, as expected for dominant negative mutations. More recently, it has been suggested that the LP is not generated by Best1 because mBest1 knockout mice have normal LPs.<sup>30</sup> There is evidence that hBest1 regulates voltage-gated  $\text{Ca}^{2+}$  channels and  $\text{Ca}^{2+}$  signaling.<sup>30,31</sup>

The expressivity of the vitelliform phenotype is variable. Although BVMD is usually described as a juvenile-onset disease, many patients do not manifest lesions until they are adults<sup>32–35</sup> and some affected individuals never have vitelliform lesions, even though they have severely depressed LPs.<sup>34</sup> In contrast to the vitelliform lesions, a reduced LP is found in almost all patients who have BVMD. However, there are several reported cases of individuals with *hBest1* mutations who have normal LPs. This raises important questions: (1) If the LP is normal in patients with *hBest1* mutations, either the mutations must not affect hBest1  $\text{Cl}^-$  channel function or else the LP is not generated by hBest1. (2) If macular degeneration occurs in patients with *hBest1* mutations that alter  $\text{Cl}^-$  channel function but these patients have normal LPs, it suggests that the reduced LP is not in the pathway that causes macular degeneration, but rather is a secondary consequence of the disease process. In this study, we addressed this question by examining the  $\text{Cl}^-$  currents that were generated by six mutations found in patients with adult-onset macular dystrophies that were not considered to be BVMD. The  $\Delta$ I295 and D312N mutations clearly

From the Department of Cell Biology and The Center for Neurodegenerative Disease, Emory University School of Medicine, Atlanta, Georgia.

Supported by National Eye Institute Grants EY014852 and National Institute of General Medical Sciences Grant GM060448.

Submitted for publication March 12, 2007; revised May 9 and June 18, 2007; accepted August 16, 2007.

Disclosure: **K. Yu**, None; **Z. Qu**, None; **Y. Cui**, None; **H.C. Hartzell**, None

The publication costs of this article were defrayed in part by page charge payment. This article must therefore be marked “advertisement” in accordance with 18 U.S.C. §1734 solely to indicate this fact.

Corresponding author: H. Criss Hartzell, Department of Cell Biology and The Center for Neurodegenerative Disease, Emory University School of Medicine, 615 Michael St., 535 Whitehead Biomedical Research Building, Atlanta, GA 30322; [criss.hartzell@emory.edu](mailto:criss.hartzell@emory.edu).

affected Cl<sup>-</sup> channel function, whereas the effects of the other mutations were subtle (E119Q and A146K) or negligible (T216I and L567F). For several of these mutations, the correlation between the Arden ratio and Cl<sup>-</sup> channel defect was poor, suggesting that hBest1 is not solely responsible for the LP.

## METHODS

The methods, described in detail previously,<sup>25,28</sup> are briefly summarized.

### Electrophysiological Methods

hBest1 tagged with the myc epitope at the C terminus in pRK5 was obtained from Jeremy Nathans, Johns Hopkins University (Baltimore, MD). Mutations were made using PCR-based mutagenesis (Quick-changer; Stratagene, La Jolla, CA). hBest1 and pEGFP (Invitrogen, Carlsbad, CA) were transfected into HEK-293 cells (5:1 ratio, 2 μg total DNA per 3.5-cm plate), using a blend of lipids (Fugene-6; Roche Molecular Biochemicals, Indianapolis, IN). Single cells identified by enhanced green fluorescent protein (EGFP) fluorescence were used for whole-cell patch clamp experiments within 72 hours. Fire-polished borosilicate glass patch pipettes were 3 to 5 MΩ. Experiments were conducted at room temperature (20–24°C). Because the liquid junction potentials were small (<2 mV), no correction was made. The standard pipette solution contained (mM) 146 CsCl, 2 MgCl<sub>2</sub>, 5 (Ca<sup>2+</sup>)-EGTA, 8 HEPES, and 10 sucrose (pH 7.3), adjusted with NMDG (*N*-methyl-D-glucamine). The zero-Ca<sup>2+</sup> pipette solution contained 5 mM EGTA without added Ca<sup>2+</sup>, whereas the high-Ca<sup>2+</sup> pipette solution contained a mixture of 5 mM EGTA and 5 mM Ca<sup>2+</sup>-EGTA to make solutions with different free [Ca<sup>2+</sup>].<sup>36</sup> In the text, high-Ca<sup>2+</sup> solution refers to Ca<sup>2+</sup> concentrations between 600 nM and 4.5 μM. The calculated Ca<sup>2+</sup> concentrations were confirmed in each solution by Fura-2 (Invitrogen-Molecular Probes, Eugene, OR) measurements using a luminescence spectrophotometer (model LS-50B; Perkin Elmer, Wellesley, MA). The standard extracellular solution contained (mM) 140 NaCl, 5 KCl, 2 CaCl<sub>2</sub>, 1 MgCl<sub>2</sub>, 15 glucose, and 10 HEPES (pH 7.4) with NaOH. This combination of intracellular and extracellular solutions set  $E_{rev}$  (the reversal potential) for Cl<sup>-</sup> currents to 0, while cation currents carried by Na<sup>+</sup> or Cs<sup>+</sup> had very positive or negative  $E_{rev}$ , respectively. When Cl<sup>-</sup> was replaced with another anion, NaCl was replaced on an equimolar basis with the Na<sup>+</sup> salt of the substitute anion. Osmolarity was adjusted with sucrose to 303 mOsm for all solutions.

### Analysis of Data

Data are expressed as the mean ± SEM. Statistical difference between means was evaluated by two-tailed *t*-test. Relative anion conductance was determined by measuring the slope of the current-voltage (*I*-*V*) curve determined from voltage ramps with different extracellular anions.<sup>25,28</sup> Relative permeability was determined by measuring the shift in  $E_{rev}$  after changing the bath solution from 151 mM Cl<sup>-</sup> to 140 mM substitute anion plus 11 mM Cl<sup>-</sup>. The permeability (*P*) ratio was calculated by using the Goldman-Hodgkin-Katz equation:

$$P_x/P_{Cl} = [Cl^-]_o/[X^-]_o \exp(\Delta E_{rev}F/RT) - [Cl^-]_o/[X^-]_o,$$

where  $\Delta E_{rev}$  is the difference between  $E_{rev}$  with the test anion X<sup>-</sup> and that observed with symmetrical Cl<sup>-</sup> and *F* (Faraday's constant), *R* (ideal gas content), and *T* (temperature in kelvin) are the thermodynamic parameters.

### Cell Surface Biotinylation

Transfected and control HEK-293 cells were placed on ice, washed three times with PBS, and biotinylated with 0.5 mg/mL sulfo-NHS-LC biotin (Pierce Chemical Co., Rockford, IL) in PBS for 30 minutes. The cells were washed, collected, and suspended in lysis buffer (250 μL 150 mM NaCl, 5 mM EDTA, 50 mM HEPES [pH 7.4], 1% Triton X-100,

0.5% protease inhibitor cocktail (cocktail III; Calbiochem, San Diego, CA), and 10 μM phenylmethylsulfonyl fluoride [PMSF] per 100-mm dish). The extract was clarified at 10,000g for 15 minutes. Biotinylated proteins were isolated by incubation of 200 μL of extract with 100 μL of streptavidin beads (Pierce Chemical Co.) overnight with gentle agitation. The beads were collected and washed four times with 0.6 mL lysis buffer + 200 mM NaCl. Bound biotinylated proteins were eluted, run on SDS-PAGE gels, and probed with anti-myc and anti-GAPDH antibodies, followed by secondary anti-mouse IgG. Immunoreactive bands were visualized by enhanced chemiluminescence (ECL kit; GE Healthcare, Piscataway, NJ).

## RESULTS

There are approximately 100 mutations in *hBest1* that have been linked to macular dystrophies (Fig. 1). We began by searching the *VMD2* database ([http://www-huge.uni-regensburg.de/VMD2\\_database/index.php?select\\_db=VMD2/](http://www-huge.uni-regensburg.de/VMD2_database/index.php?select_db=VMD2/)) provided in the public domain by the Institute of Human Genetics, University of Regensburg, Germany) for mutations that were found in patients with macular dystrophies other than BVMD or in BVMD patients having normal or near-normal EOGs. The mutations that potentially fall into these categories are listed in Table 1. First, we wanted to know whether macular dystrophies other than BVMD caused by *hBest1* mutations were also associated with defects in Cl<sup>-</sup> channel function. Second, we wanted to know whether mutations associated with macular degeneration in patients with normal EOGs produce less severe Cl<sup>-</sup> channel defects.

### ΔI295

We first examined ΔI295 which is a common juvenile-onset BVMD-causing mutation<sup>2,3,41</sup> located in a very highly conserved motif immediately after the last predicted transmembrane domain of hBest1 (Table 1, Fig. 1).<sup>21,37,38</sup> Patients with the ΔI295 mutation usually have a depressed LP. However, it was recently reported that two patients with pseudohypopyon or vitelliruptive lesions had perfectly normal EOGs.<sup>41</sup> Although the EOGs eventually became abnormal after 4 to 5 years, the observation that the abnormal EOG follows, rather than precedes the vitelliform lesion challenges the hypothesis that BVMD is directly caused by a defect in the LP. I295 is located within a region that is a hot spot for BVMD-causing mutations. Mutations in 14 of the 19 amino acids between positions 293 and 312 are associated with BVMD. Sun et al.<sup>20</sup> tested the Cl<sup>-</sup> channel activity of several of these (G299E, E300D, D301E, and T307I) and reported that they were non-functional. Several were dominant negative.

As shown in Figure 2A, ΔI295 induced negligibly small currents when transfected alone, and it inhibited WT currents when cotransfected with WT hBest1. Thus, the ΔI295 mutation resembles many of the other disease-causing mutations that are associated with juvenile-onset BVMD.<sup>20</sup> To determine whether the absence of Cl<sup>-</sup> current was due to an inability of the protein to be trafficked to the plasma membrane, we tested the trafficking of ΔI295 using membrane biotinylation. Figure 2B shows that biotinylated fractions from the ΔI295-transfected cells had a 68-kDa band corresponding to hBest1. Thus, ΔI295 channels are trafficked normally into the plasma membrane. To be certain that the biotinylation reaction did not label intracellular proteins, biotinylated proteins were immunoblotted with an antibody against GAPDH, a cytosolic protein. As expected if the biotinylation labeled only cell surface proteins, the 37-kDa GAPDH bands were found only in the total lysate and were not present in the biotinylated fraction (Fig. 2B).

Because HEK cells are not derived from RPE cells, we also tested WT and ΔI295 hBest1 in RPE-J cells, which is a cell line



TABLE 1. VMD2 Mutations in Patients with Various Maculopathies

Mutation	Diagnosis	Family History	EOG*	Ref.	Cl <sup>-</sup> Current % WT§
T6P	AVMD	No		3	<20%, Ref. 20
R47H	AVMD	No		3	
R105C	AMD	No		32	
E119Q	Bull's eye maculopathy AMD	No	? 1.0†	4, 32, 39	Like WT¶
A146K	AVMD	Yes	1.0-1.5	4, 39	~30%¶
L149X	AMD	Yes		32	
T216I	AMD	No	3.2-3.4	4, 39	Like WT¶
A243V	BVMD AVMD	Yes	1.1-1.9	3, 40	<20%, Ref. 28
V275I	AMD	No		32	
ΔI295	BVMD	Yes	1.0-2.9	2, 3, 41	Nonfunctional Dominant negative¶
D312N	AVMD	Yes	1.3‡	3	Nonfunctional Dominant negative¶
L567F	AMD	No	2.0-3.2	4, 39	Like WT¶

\* Values less than 1.5 are considered pathological.

† Described in one patient with AMD by Lotery et al.<sup>32</sup>

‡ Personal communication, B.H.K. Weber.

§ 1 to 2 days after transfection

|| Not studied because these mutations were found in sporadic cases with no family history and EOG data not available.

¶ This study.

hBest1+hBest2 channels as it does on homomeric hBest1 channels. Sun et al.<sup>20</sup> have shown by chemical cross-linking that hBest1 and hBest2 can form heteromeric channels.

We examined the ability of another hBest1 mutant (G222E) to suppress hBest2 currents. The G222E mutation is linked to classic juvenile-onset BVMD with complete penetrance and expressivity of a reduced LP.<sup>29</sup> When transfected alone in HEK cells, G222E did not induce any currents but was highly expressed on the membrane (data not shown). In contrast to ΔI295, G222E suppressed currents generated by either hBest1 or hBest2 (Figs. 3C, 3D). These results demonstrate that hBest1 can form heteromeric channels with hBest2 but that the ΔI295 mutant does not have a dominant negative effect on the heteromeric channel. Thus, the normal LP in some patients with ΔI295 may be explained by upregulation of hBest2 in some patients with I295. Stohr et al.<sup>42</sup> report that hBest2 is expressed in RPE as determined by RT-PCR, but it remains speculative whether hBest2 can compensate for hBest1 dysfunction in the ΔI295 mutants.

### D312N

The D312N mutation was chosen because it is located in the same highly conserved motif as ΔI295 (Fig. 1) but is linked to AVMD rather than BVMD (Table 1). Because D312N was identified in a patient with AVMD and not BVMD, we expected that D312N might have a milder Cl<sup>-</sup> channel phenotype. However, the D312N mutation was both nonfunctional and dominant negative. As shown in Figure 4A, D312N induced negligibly small currents when transfected alone and it inhibited WT currents when cotransfected with WT hBest1. To determine whether the absence of Cl<sup>-</sup> current was due to the inability of the protein to be trafficked to the plasma membrane, we tested the trafficking of D312N by using membrane biotinylation. Figure 4B shows that the D312N mutant was effectively trafficked to the plasma membrane.

The D312N mutation was described in a patient with AVMD who had a family history of macular degeneration.<sup>3</sup> EOG data were not reported in by the authors for the D312N mutation, but EOG data on one patient (A-3) were provided by Bernhard H. F. Weber (personal communication, August 10, 2006), who stated, "Patient HN (A-3) had an EOG at age 46 of 1.34/1.36 (right/left). At age 55 the EOG responses were 1.30/1.33

(right/left). The scale of the responses is such that below 1.50 the EOG is regarded subnormal or pathologic." Although the LP is subnormal, it is not absent, as would be expected if the LP was generated solely by hBest1. The data also raise a question about the universality of using the EOG as a rigid diagnostic indicator for AVMD and BVMD, because some patients with hBest1 mutations may have near-normal LPs.

### A146K

A146K is linked to AVMD<sup>4,39</sup> and is located in a cytoplasmic loop after the second transmembrane domain (Table 1, Fig. 1). The LP in these patients was significantly depressed. When A146K was transfected into HEK cells, the Cl<sup>-</sup> current was much smaller than the WT currents. In several different experiments, the amplitude ranged from 20% to 40% of the WT current (Fig. 5A). Unlike the D312N and ΔI295 mutations, which are clearly nonfunctional, the A146K mutation produced measurable currents. Coexpression of the A146K mutation with WT hBest1 had no effect on the hBest1 currents (Fig. 5A). The A146K mutation is similar to the A243V mutation that we have described previously.<sup>28</sup> In both mutants, Cl<sup>-</sup> channel functionality is reduced, but the protein is not dominant negative. This supports our idea that adult onset of disease in A146K patients might be explained by a gene dosage effect. In some individuals, the presence of the WT allele may postpone the onset of disease symptoms. The depressed LP is consistent with the reduced Cl<sup>-</sup> current amplitudes. In addition, the relative anion permeability of the A146K channels is different from WT (Table 2). SCN is more permeant through the A146K channels than through WT channels. Whether this change in selectivity has any pathophysiological consequence remains unknown.

### E119Q

The E119Q mutation was chosen for analysis because it was found in patients with Bull's-eye maculopathy and AMD<sup>4,32,39</sup> (Table 1). This mutation is predicted to be located in a cytoplasmic loop (Fig. 1). As shown in Figure 6A, the E119Q currents were similar in amplitude to WT currents. However, the channels exhibited altered anionic permeability for SCN relative to Cl<sup>-</sup> (Table 2).

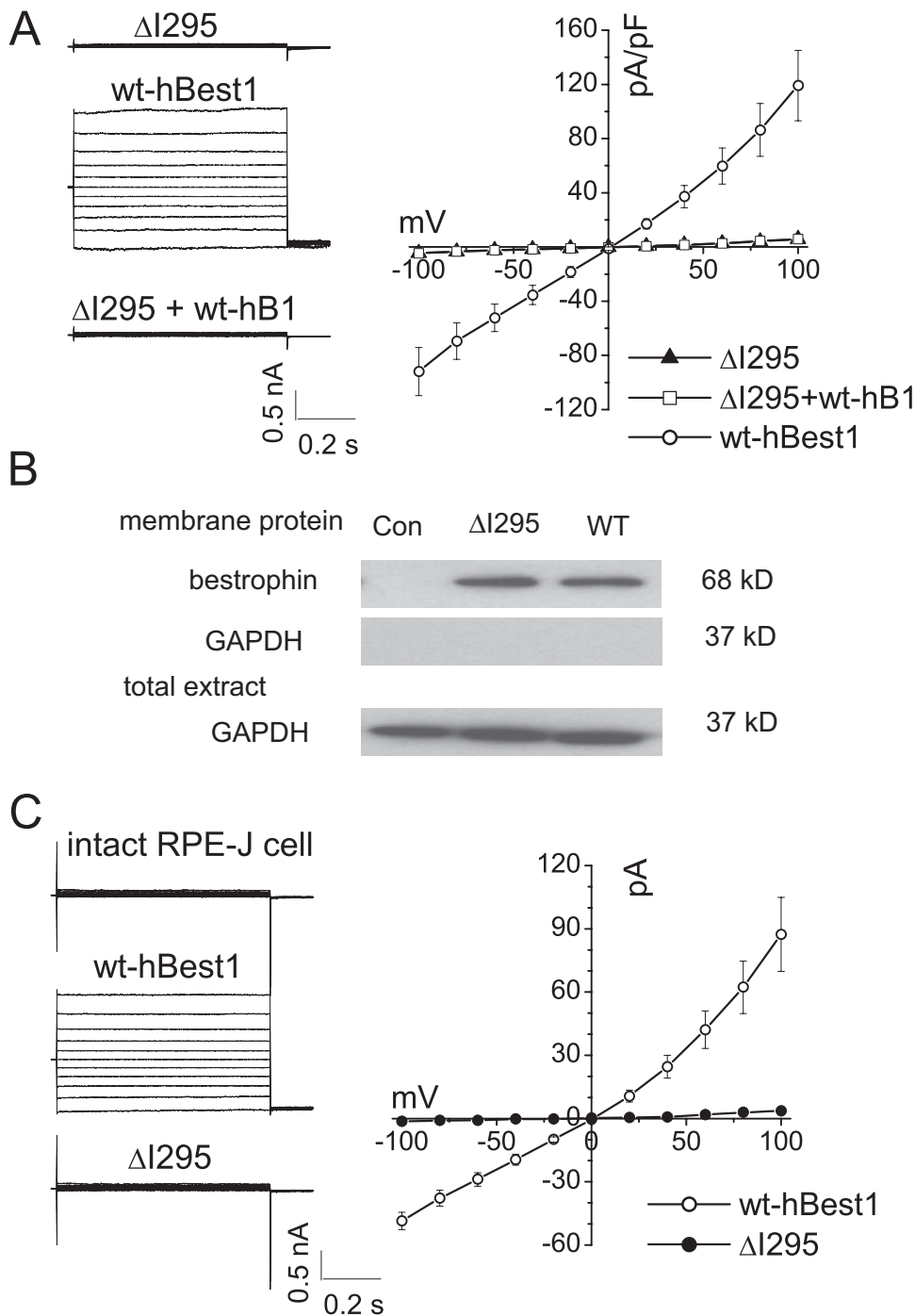


**FIGURE 2.** hBest1  $\Delta I295$  mutant is nonfunctional and dominant negative on WT hBest1. (A) Representative current traces (left) and mean *I-V* relationships (right) for  $\Delta I295$  mutant alone, WT and cotransfected WT, and mutant hBest1.  $\Delta I295$  mutant significantly inhibited the WT current ( $P < 0.005$ , two-tailed *t*-test) and the inhibition was dominant negative. Each data point represents at least seven cells. (B) Localization of  $\Delta I295$  mutant hBest1 in the plasma membrane of HEK-293 cells was tested. Biotinylated membrane proteins were probed with antibodies to the myc tag on hBest1 (68-kDa band) and to GAPDH (37 kDa band), respectively. (C) Representative current traces (left) and mean *I-V* relationships (right) of untransfected RPE-J cells and RPE-J cells transfected with WT hBest1 or  $\Delta I295$  hBest1.

There are at least two patients in the literature with the E119Q mutation. The patients had no known family history of eye disease. One had a diagnosis of AMD, but had no LP.<sup>32</sup> The observation that the E119Q mutation produced normal-amplitude  $Cl^-$  currents is inconsistent with the absent LP in this patient. This inconsistency suggests that hBest1 is not the channel responsible for generating the LP. Although the anionic selectivity of the channel is altered by the mutation, it does not seem likely that this could account for the absent LP. The other E119Q cases had a diagnosis of Bull's eye maculopathy,<sup>4,39</sup> but EOG data were not reported.

### L567F

We then tested the L567F mutation because this mutation was found in a patient with age-related macular degeneration

(AMD), and the patient had a normal EOG (Table 1).<sup>4,39</sup> L567F is located in the distal C terminus of hBest1 and is one of only four potential disease-causing mutations that have been described beyond amino acid 312. We expressed L567F in HEK-293 cells and compared the biophysical properties with WT hBest1. The *I-V* relationships in Figure 7A show that the mutant induced a current with similar amplitude and properties as WT currents. The L567F-induced current exhibited an anionic permeability order of  $SCN^- > I^- > Br^- > Cl^-$  and a relative conductance order of  $SCN^- > I^- > Br^- > Cl^-$ , which were not significantly different from WT (Figs. 7B, 7C; Table 2). Because L567F was found in a single sporadic patient with AMD, the question arises as to whether this mutation is actually a disease-causing mutation or a benign polymorphism. This issue has been discussed in an article by Allikmets et al.<sup>4</sup>

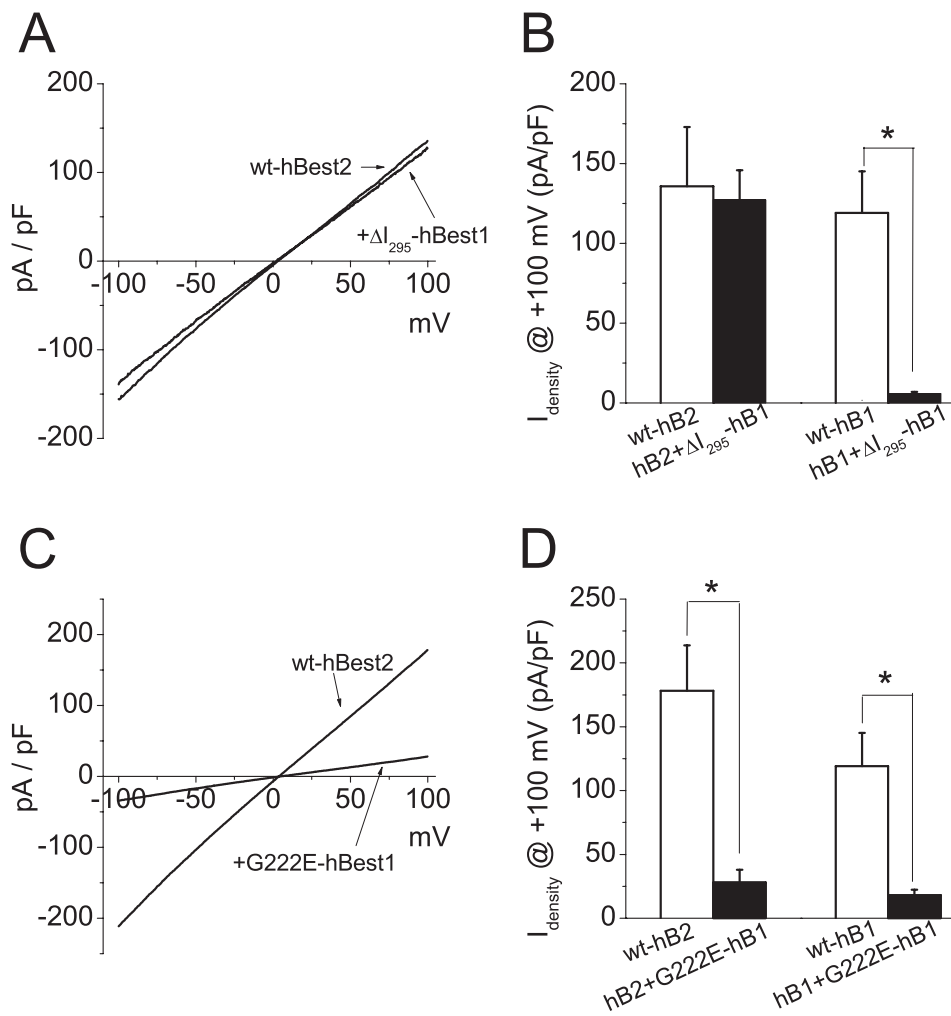


**FIGURE 3.** Dominant negative effects of hBest1 mutants  $\Delta$ I295 and G222E on WT hBest1 and hBest2. (A) Mean I-V relationships recorded with high  $[Ca^{2+}]_i$  from WT hBest2-transfected HEK cells and cells cotransfected with  $\Delta$ I295-hBest1 and WT hBest2. (B) Mean current densities for hBest1 and hBest2 currents in the presence and absence of coexpression with  $\Delta$ I295-hBest1. (C) Mean I-V relationships recorded with high  $[Ca^{2+}]_i$  from WT hBest2-transfected HEK cells and the cells cotransfected with G222E-hBest1 and WT hBest2. (D) Mean current densities at +100 mV for hBest1 and hBest2 currents in the presence (■) and absence (□) of coexpressed  $\Delta$ I295-hBest1.

## T216I

We studied the T216I mutation because it was found in two patients with AMD who had normal EOGs. The topological location of T216 is ambiguous. The model of Tsunenari et al.<sup>21</sup> places it in an extracellular loop, whereas the models of Marmorstein and Kinnick<sup>37</sup> and Milenkovic et al.<sup>38</sup> locate it cytoplasmically. It is located between two highly conserved regions, but it is not itself highly conserved. It is in one of the hot spots for hBest1 mutations: 24 mutations have been reported between positions 206 and 243.

The current amplitudes and properties for the T216I mutant were not statistically different from WT (Fig. 8A, 8B). The T216I mutation did not affect the maximum amplitude of current with high  $[Ca^{2+}]_i$  (>600 nM; Fig. 8C) and the relative anion conductances and permeabilities were the same as WT (Table 2). At low  $[Ca^{2+}]_i$  (close to the resting level), the T216I mutation produced a slightly higher channel activity than did the WT channel (Fig. 8C). The Cl<sup>-</sup> channel properties of this mutant correspond with the normal EOG of patients who have this mutation (Table 1).

## DISCUSSION

### Cl<sup>-</sup> Channel Dysfunction of hBest1 Mutants

All 18 human disease-causing hBest1 mutations that have been examined in prior studies exhibit defective Cl<sup>-</sup> channel function.<sup>20,21,28,29</sup> We add  $\Delta$ I295, D312N, E119Q, and

A146K to that list. The only mutations yet described to have apparently normal Cl<sup>-</sup> channel function are T216I and L567F. The mutations that we examined were all expressed on the plasma membrane as determined by membrane biotinylation. Approximately 40% to 50% of the protein was on the plasma membrane relative to the cytoplasm and the value was similar for all mutations that we studied. The specific levels were: 42.6% for WT hBest1, 48.0% for E119Q, 50.8% for A146K, 45.2% for  $\Delta$ I295, and 48% for D312N. The presence of a significant fraction of hBest1 in intracellular membranes could be an artifact of overexpression or could suggest that hBest1 plays a role in intracellular compartments. We have preliminary data that a significant fraction of bestrophin is in intracellular membranes in native cells, suggesting that the intracellular location is not a consequence of overexpression.

A brief comment on the use of HEK-293 cells as the expression system may be appropriate. It could be argued that an RPE cell line would be a better choice than HEK cells, because the RPE cell line may be more likely to express partners or factors that are essential for bestrophin function or expression. However, because expressed bestrophin currents are identical in HEK, HeLa, and ARPE-19 cells,<sup>23</sup> HEK cells seem to have everything that the RPE cell line has. Furthermore, RPE cell lines remain rather undifferentiated unless they are grown as a confluent monolayer in air interfacial conditions. Because single isolated cells are necessary for voltage clamp, the use of well-differentiated

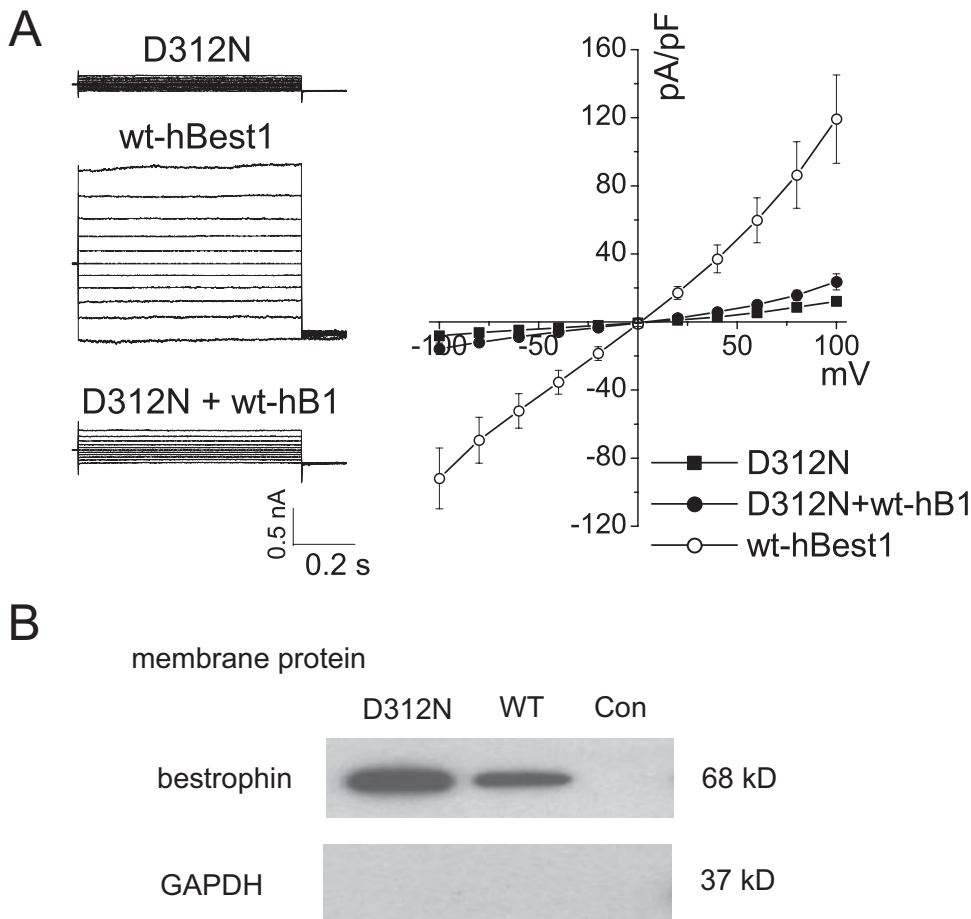


**FIGURE 4.** Dominant negative effects of D312N mutant on WT hBest1. A cell was voltage clamped with 750-ms duration steps in 20-mV increments from  $-100$  to  $+100$  mV with  $4.5 \mu\text{M}$  (high) free  $[\text{Ca}^{2+}]_i$ . **(A)** Representative current traces (*left*) and mean current-voltage (*I-V*) relationships (*right*) for D312N mutant alone, WT and cotransfected WT, and mutant hBest1. D312N mutant significantly inhibited the WT current ( $P < 0.005$ , two-tailed *t*-test) and the inhibition was dominant negative. Each data point represents at least seven cells. **(B)** Localization of D312N mutant hBest1 in the plasma membrane of HEK-293 cells. Biotinylated proteins (*top*) from nontransfected (control), WT, and D312N mutant hBest1-transfected cells were probed with antibody to the myc tag on hBest1 (68-kDa band). Biotinylated membrane proteins (*bottom*) were probed with antibody to intracellular protein GAPDH (37-kDa band) to show that the biotinylation reaction labeled only cell surface proteins.

RPE cells is not compatible with overexpression and patch clamp analysis.

The  $\text{Cl}^-$  channel properties of three (T216I, L567F, and A146K) of the six mutations we examined in this article correlated well with the EOG values found in patients with these mutations. The T216I and L567F mutants had WT  $\text{Cl}^-$  currents and were found in patients who had normal EOGs. The A146K mutant was defective in  $\text{Cl}^-$  channel function and was found in patients with clearly subnormal EOGs. It should be noted that the number of patients for which EOG data is available is limited for these mutations (one patient for A146K, two patients for T216I, and two patients for L567F). The finding that T216I and L567F mutants had no effect on the EOG or  $\text{Cl}^-$  channel function raises the question of whether these mutations are actually disease-causing. Neither mutation is associated with a family history of disease and neither mutation is a highly conserved residue. The possibility should be considered that these two mutations are benign polymorphisms. If this is the case, it means that of the 25 disease-associated mutations that we and others have examined, all of them cause disease by interfering with  $\text{Cl}^-$  channel function. Whether this will hold true for all the other  $\sim 80$  mutations that have not yet been examined remains to be seen. However, it suggests that  $\text{Cl}^-$  channel dysfunction is a major disease mechanism.

The severity of the  $\text{Cl}^-$  channel defect in the other three mutations (E119Q, D312N, and  $\Delta$ I295) did not obviously correlate with the Arden ratio. The E119Q channels appear normal when expressed in HEK cells, but the only patient with this mutation for which EOG data are available had no LP. The D312N mutant was nonfunctional as a  $\text{Cl}^-$  channel and was dominant negative, but at least one patient with this

mutation had a measurable, but subnormal, LP. And, although the  $\Delta$ I295 mutation was nonfunctional and dominant negative, at least three individuals with this mutation had a normal LP, although other individuals with the  $\Delta$ I295 mutation had no LP. Although the number of patients for which EOG data are available for these three mutations is limited (one for E119Q, one for D312N, and three for  $\Delta$ I295), these data raise questions about whether hBest1 generates the LP. The normal LP in some patients could be explained if the LP is not generated by bestrophin, as suggested by Marmorstein et al.<sup>30</sup> In this case, the decreased LP would be secondary to the hBest1  $\text{Cl}^-$  channel defect. Another possibility is that the patients with vitelliform lesions and normal LPs have a compensatory conductance that maintains the LP within normal levels for a period even though transport across the RPE is abnormal. We tested this possibility for the D312N and G222E mutations and found that D312N was not dominant negative on WT hBest2 channels, whereas G222E was dominant negative. Thus, if hBest2 is expressed in RPE,<sup>42</sup> hBest2 might compensate for the loss of hBest1 function in D312N mutants but not G222E mutants. Whether such a mechanism actually accounts for the difference in these mutations remains to be tested.

The fact that *hBest1* mutations were found in patients with BVMD, AVMD, Bull's-eye maculopathy, and AMD suggests that different *hBest1* mutations can produce diseases that differ in their morphologic and pathologic features. In general, mutations that cause juvenile-onset BVMD are both nonfunctional and dominant negative on hBest1. In contrast, mutations that produce adult-onset disease generally have less severe effects on  $\text{Cl}^-$  channel function: some mutants have apparently nor-

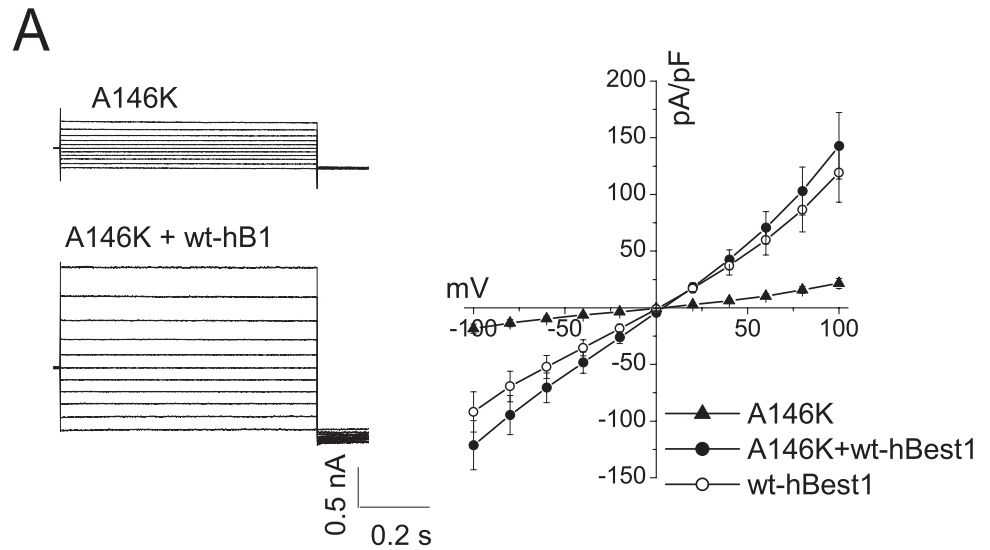


**FIGURE 5.** Expression of A146K mutant hBest1 in HEK cells. **(A)** Representative current traces (*left*) and mean current-voltage (*I-V*) relationships (*right*) for A146K mutant alone and cotransfected WT and mutant hBest1. **(B)** Localization of A146K mutant hBest1 in the plasma membrane of HEK-293 cells (24 hours after transfection). Biotinylated membrane proteins were probed with antibodies to the myc tag on hBest1 (68-kDa band) and to GAPDH (37-kDa band).

mal Cl<sup>-</sup> channel function, and others have residual Cl<sup>-</sup> current and are not dominant negative.

### Mechanisms of BVMD and Variability of Age of Onset

If mutations in *hBest1* produce retinal disease by disrupting the Cl<sup>-</sup> channel functions of hBest1, how does the dysfunction of a Cl<sup>-</sup> channel result in macular degeneration? If transepithelial transport across the RPE is disrupted by mutations in hBest1, one would expect that the ionic composition and volume of the fluid between the RPE and the photoreceptor outer segments would be altered. This change in subretinal fluid would very likely alter the interaction between RPE and photoreceptors. In support of the suggestion that BVMD is a consequence of altered RPE-photoreceptor interaction is the observation

that a common feature of BVMD is a separation of the neural retina from the RPE. This was recognized in early studies<sup>8</sup> but perhaps has become more obvious from recent studies in which optical coherence tomography was used to visualize the retina.<sup>7,9-11</sup> These recent studies have demonstrated cystic spaces both between the neural retina and RPE and also below the RPE. The RPE plays several very important roles in the retina including regeneration of visual pigment and photoreceptor turnover. Regeneration of visual pigment involves transport of retinoids between the photoreceptors and RPE through the subretinal space. In photoreceptor turnover, RPE phagocytose an enormous quantity of photoreceptor outer segments each day and degrade them in phagolysosomes. A change in RPE-photoreceptor interface would be likely to affect both of these processes. Changes in the traffic of retinoids in the visual

**TABLE 2.** Anionic Selectivity of Various *hBest1* Mutants

	$G_X/G_{Cl}$				$P_X/P_{Cl}$			
	Cl	Br	I	SCN	Cl	Br	I	SCN
WT	1	1.12 ± 0.03	1.2 ± 0.13	2.06 ± 0.26	1	1.95 ± 0.11	3.49 ± 0.29	4.49 ± 0.51
Mutants								
E119Q	1	1.06 ± 0.03	1.16 ± 0.07	1.95 ± 0.16	1	1.69 ± 0.1	3.23 ± 0.33	8.9 ± 1.03*
A146K	1	1.1 ± 0.05	0.84 ± 0.13	1.71 ± 0.41	1	2.33 ± 0.56	3.9 ± 0.45	14.11 ± 1.87*
T216I	1	1.16 ± 0.04	1.25 ± 0.1	1.7 ± 0.24	1	1.77 ± 0.11	3.02 ± 0.18	7.11 ± 0.96
L567F	1	1.22 ± 0.06	1.37 ± 0.14	2.24 ± 0.29	1	1.71 ± 0.04	3.32 ± 0.35	6.51 ± 1.06

$G_X/G_{Cl}$  is conductance of anion *X* relative to Cl<sup>-</sup> measured as the slope of the current-voltage (*I-V*) relationship near the reversal potential.  $P_X/P_{Cl}$  is the permeability of anion *X* relative to Cl<sup>-</sup> measured as the shift in the reversal potential and the Goldman-Hodgkin-Katz equation. For details see Refs. 23-25. D312N and ΔI295 are not included because the currents were too small for analysis.

\* Statistically different from WT at  $P < 0.01$ .

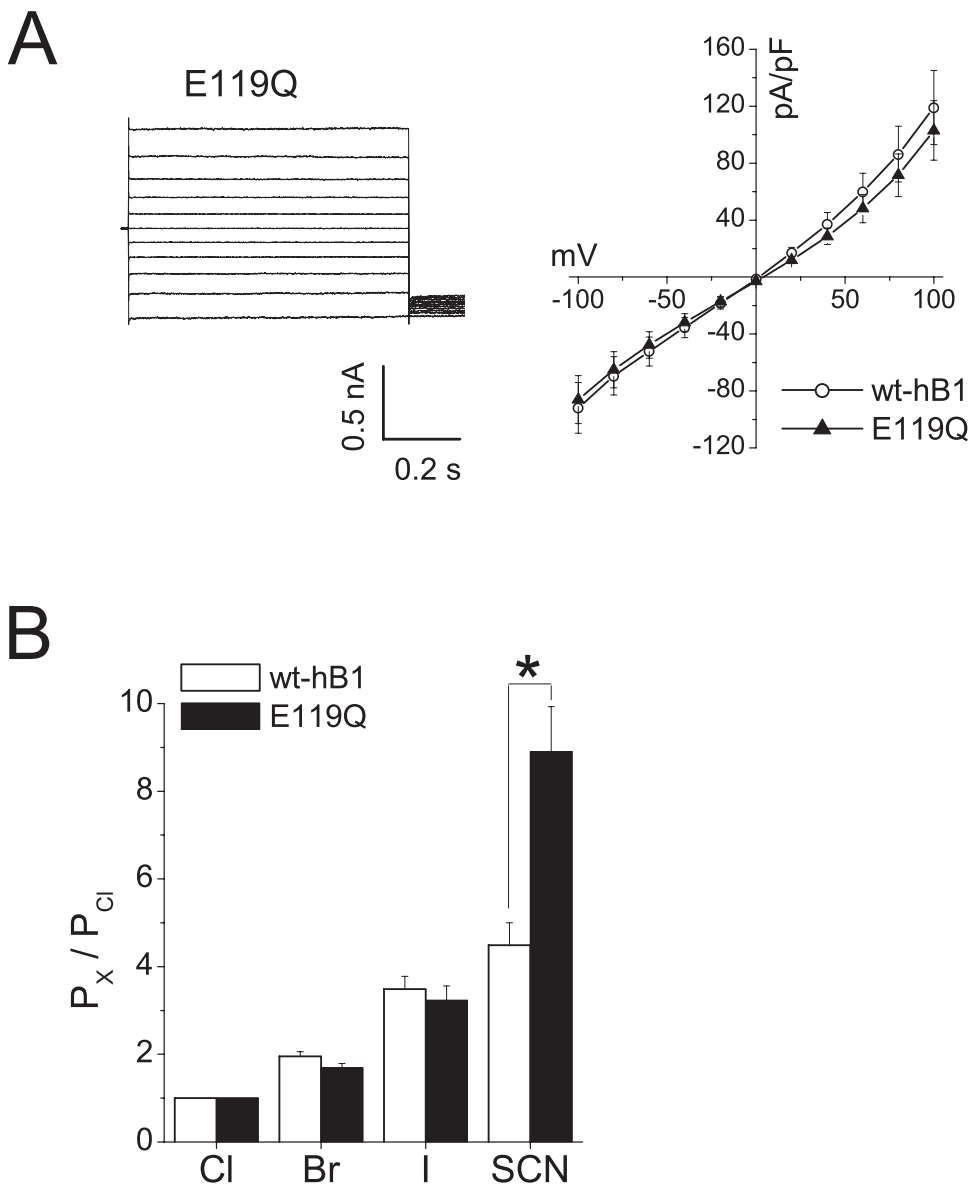


**FIGURE 6.** Altered anion permeability of E119Q hBest1. **(A)** Representative E119Q-hBest1 induced current traces (*left*) and respective mean *I-V* relationships (*right*) with high  $[Ca^{2+}]_i$ . Each averaged point represents data from at least 7 cells. **(B)** The relative permeability ratios with the extracellular anions,  $Cl^-$ ,  $Br^-$ ,  $I^-$ , or  $SCN^-$  were calculated from the Goldman-Hodgkin-Katz equation. Each data point represents at least seven cells.

cycle or outer segments in photoreceptor turnover would be likely to contribute to deposition of pigment and formation of vitelliform lesions.

Although BVMD was initially described as having a juvenile age of onset, as more mutations and more patients have been examined, it has become clear that the age of onset is variable (e.g., Ref. 34). This variability could develop as a result of differences in the  $Cl^-$  channel phenotype, for example, whether the mutation is dominant negative or not. For mutations that are not dominant negative, the WT allele may preserve normal visual function until a later age. Disease progression is likely to be a multistep process in which photoreceptor-RPE interactions are first compromised by defective transepithelial ion transport, and then vitelliform lesions develop secondarily by processes that may be dependent on variations in, for example, retinoid biochemistry or phagocytosis.

## CONCLUSIONS

Of the 25 hBest1 mutations that have been examined, all of them except L567F and T216I produce some abnormality in  $Cl^-$  channel function. Strong evidence for hBest1 mutations

producing vitelliform lesions in the absence of EOG abnormalities exists only for the  $\Delta I295$  and A243V mutations. Less compelling but supportive evidence also exists for the D312N and E119Q mutations. These data support the suggestion of Marmorstein et al.<sup>30</sup> that hBest1 is not the sole generator of the LP. The most compelling evidence against a role for hBest1 in generating the LP is that at saturating illumination the LP is normal amplitude in WT mice and in mice with the mBest1 gene disrupted (mBest1<sup>-/-</sup> mutant).<sup>30</sup> Marmorstein et al.<sup>30,43</sup> and Rosenthal et al.<sup>31</sup> have proposed that hBest1 regulates the LP indirectly via its effects on voltage-gated  $Ca^{2+}$  channels. One wonders whether the hBest1 mutations that do not alter  $Cl^-$  channel function may alter the ability of hBest1 to regulate Ca channels. If so, it is possible that mutations that affect  $Cl^-$  channel function may produce different disease phenotypes than mutations that affect the regulation of Ca channels.

There are significant parallels between macular degeneration caused by mutations in hBest1 and cystic fibrosis caused by mutations in CFTR.<sup>44</sup> In both diseases, mutations distributed throughout the protein have been linked to disease. With CFTR, and presumably hBest1, this reflects the fact that the protein has multiple functional domains that are

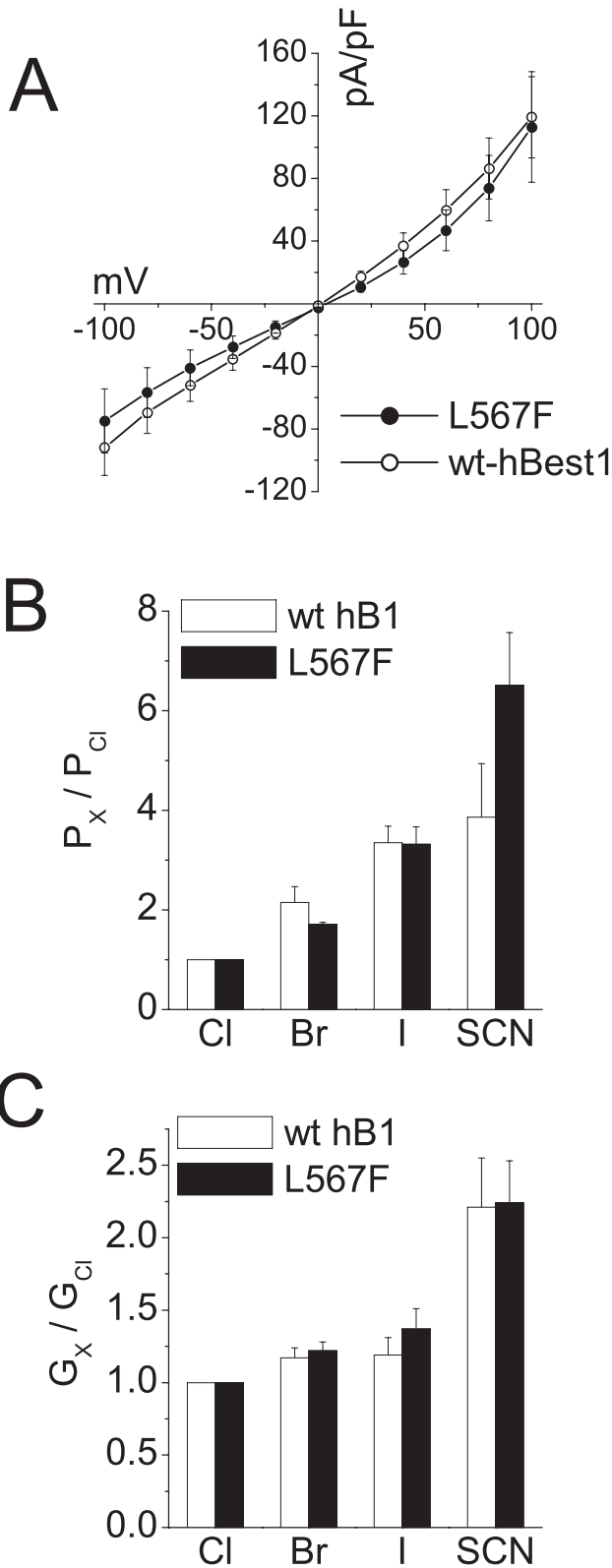


**FIGURE 7.** L567F mutant behaved like WT hBest1. (A) Mean *I-V* relationships with high intracellular [Ca<sup>2+</sup>]<sub>i</sub> for WT and L567F hBest1. The difference was not statistically significant (*P* > 0.05, two-tailed *t*-test). The relative permeability ratios (B) and mean relative conductance ratios (C) with the extracellular anions, Cl<sup>-</sup>, Br<sup>-</sup>, I<sup>-</sup>, or SCN<sup>-</sup> were calculated from the Goldman-Hodgkin-Katz equation. Each data point represents at least seven cells.

important for protein function. CFTR mutations in the nucleotide binding domains, regulatory domain, or transmembrane pore domains can cause loss of Cl<sup>-</sup> channel function by a variety of mechanisms, including defects in protein

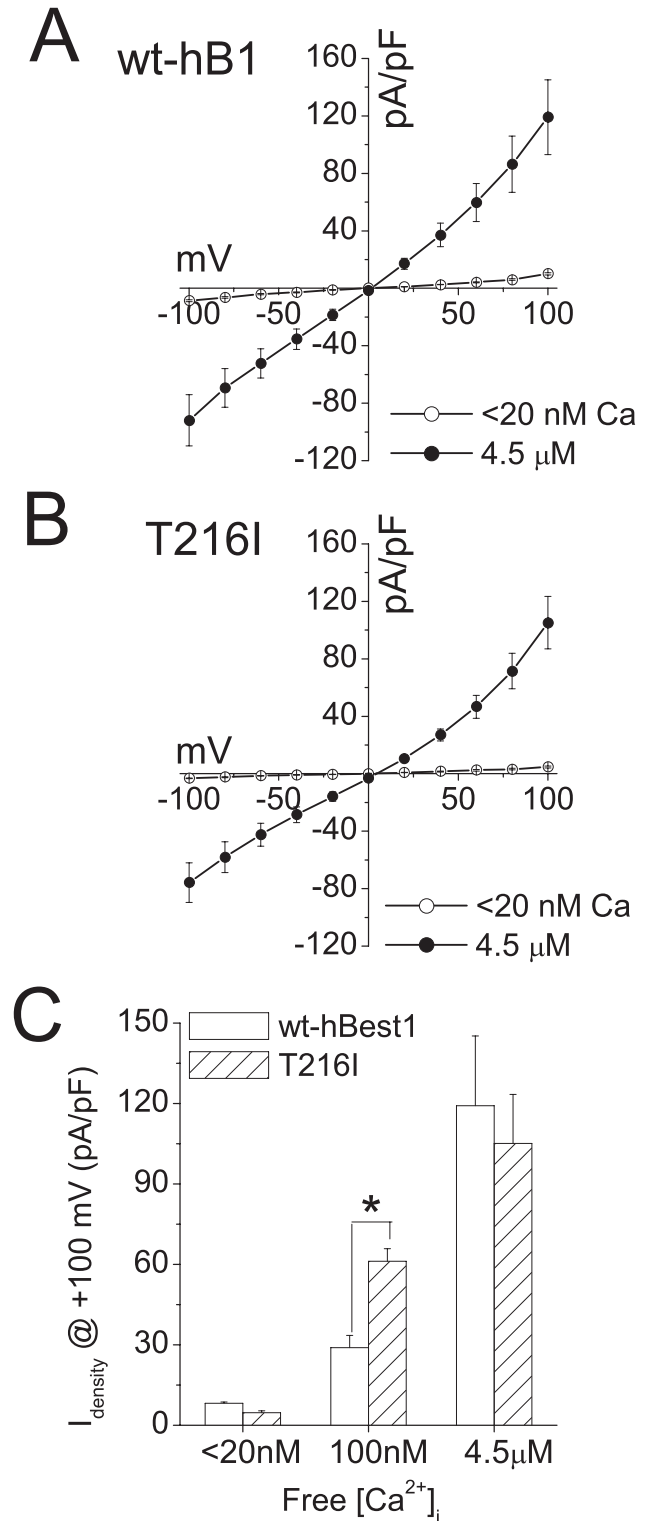


**FIGURE 8.** Higher channel activity of T216I mutant hBest1 currents in response to low level [Ca<sup>2+</sup>]<sub>i</sub> compared to WT. Mean *I-V* relationships obtained from WT (A) and T216I (B) hBest1-transfected cells with free [Ca<sup>2+</sup>]<sub>i</sub> of <20 nM and 4.5 μM. (C) The averaged current densities at +100 mV from WT (□) and T216I (▨) hBest1 were plotted at <20 nM, ~100 nM, and 4.5 μM [Ca<sup>2+</sup>]<sub>i</sub>. Averaged data represent at least seven cells.

production, processing, targeting, turnover, regulation, and conduction.

Both hBest1 and CFTR are multifunctional proteins. They are both  $\text{Cl}^-$  channels that also regulate other membrane proteins. Frequently, in CFTR there is good correlation between disease phenotype and  $\text{Cl}^-$  channel function. However, the severity of disease varies with the organ, possibly depending on the functional requirement of CFTR in that organ. The disease phenotype is often related to disorders in regulatory functions of CFTR; however, to date there are no CFTR disease-causing mutations that affect only the regulatory function without affecting the  $\text{Cl}^-$  channel as well.

With both diseases, variability in disease severity and age of onset are observed, not only with different genotypes, but also within a single genotype. Phenotype variability within a single genotype suggests that other genetic and environmental factors can modify the disease. Evidence of the existence of genetic modifiers of CF phenotypes has been found in both mice and humans.

### Acknowledgments

The authors thank Li-Ting Chien for helpful comments and discussion.

### References

- Petrukhin K, Koisti MJ, Bakall B, et al. Identification of the gene responsible for Best macular dystrophy. *Nat Genet.* 1998;19:241-247.
- Marquardt A, Stohr H, Passmore LA, et al. Mutations in a novel gene, VMD2, encoding a protein of unknown properties cause juvenile-onset vitelliform macular dystrophy (Best's disease). *Hum Mol Genet.* 1998;7:1517-1525.
- Kramer F, White K, Pauleikhoff D, et al. Mutations in the VMD2 gene are associated with juvenile-onset vitelliform macular dystrophy (Best disease) and adult vitelliform macular dystrophy but not age-related macular degeneration. *Eur J Hum Genet.* 2000;8:286-292.
- Allikmets R, Seddon JM, Bernstein PS, et al. Evaluation of the Best disease gene in patients with age-related macular degeneration and other maculopathies. *Hum Genet.* 1999;104:449-453.
- Yardley J, Leroy BP, Hart-Holden N, et al. Mutations of VMD2 splicing regulators cause nanophthalmos and autosomal dominant vitreoretinopathopathy (ADVIRC). *Invest Ophthalmol Vis Sci.* 2004;45(10):3683-3689.
- Gass DJM. Diagnosis and treatment. *Stereoscopic Atlas of Macular Diseases.* St. Louis: Mosby; 1997;1:303-313.
- Pianta MJ, Aleman TS, Cideciyan AV, et al. In vivo micropathology of Best macular dystrophy with optical coherence tomography. *Exp Eye Res.* 2003;76:203-211.
- Jaffe GJ, Schatz H. Histopathologic features of adult-onset foveomacular pigment epithelial dystrophy. *Arch Ophthalmol.* 1988;106:958-960.
- Men G, Batioglu F, Ozkan SS, Atilla H, Ozdamar Y, Aslan O. Best's vitelliform macular dystrophy with pseudohypopyon: an optical coherence tomography study. *Am J Ophthalmol.* 2004;137:963-965.
- Pierro L, Tremolada G, Intorini U, Calori G, Brancato R. Optical coherence tomography findings in adult-onset foveomacular vitelliform dystrophy. *Am J Ophthalmol.* 2002;134:675-680.
- Vedantham V, Ramasamy K. Optical coherence tomography in Best's disease: an observational case report. *Am J Ophthalmol.* 2005;139:351-353.
- Arden GB. Alterations in the standing potential of the eye associated with retinal disease. *Trans Ophthalmol Soc UK.* 1962;82:63-72.
- Deutman AF. Electro-oculography in families with vitelliform dystrophy of the fovea: detection of the carrier state. *Arch Ophthalmol.* 1969;81:305-316.
- Francois J, De Rouck A, Fernandez-Sasso D. Electro-oculography in vitelliform degeneration of the macula. *Arch Ophthalmol.* 1967;77:726-733.
- Theischen M, Schilling H, Steinhorst UH. EOG bei adulter vitelliformer Makuladegeneration (AVMD) schmetterlingsformiger Pat-terndystrophie und Morbus Best. *Ophthalmologie.* 1997;94:230-233.
- Gallemore RP, Hughes BA, Miller SS. Retinal pigment epithelial transport mechanisms and their contributions to the electroretinogram. *Prog Retinal Eye Res.* 1997;16:509-566.
- Gallemore RP, Hughes BA, Miller SS. Light-induced responses of the retinal pigment epithelium. In: Marmor MF, Wolfensberger TJ, ed. *The Retinal Pigment Epithelium.* Oxford, UK: Oxford University Press; 1998:175-198.
- Hughes BA, Gallemore RP, Miller SS. Transport mechanisms in the retinal pigment epithelium. In: Marmor MF, Wolfensberger TJ, ed. *The Retinal Pigment Epithelium.* Oxford, UK: Oxford University Press; 1998:103-134.
- Peterson WM, Meggyesy CF, Yu KF, Miller SS. Extracellular ATP activates calcium signaling, ion, and fluid transport in retinal pigment epithelium. *J Neurosci.* 1997;17:2324-2337.
- Sun H, Tsunenari T, Yau K-W, Nathans J. The vitelliform macular dystrophy protein defines a new family of chloride channels. *Proc Natl Acad Sci USA.* 2002;99:4008-4013.
- Tsunenari T, Sun H, Williams J, et al. Structure-function analysis of the bestrophin family of anion channels. *J Biol Chem.* 2003;278:41114-41125.
- Qu Z, Hartzell HC. Two bestrophins cloned from *Xenopus laevis* Oocytes express Ca-activated  $\text{Cl}^-$  currents. *J Biol Chem.* 2003;278:49563-49572.
- Qu Z, Fischmeister R, Hartzell HC. Mouse bestrophin-2 is a bona fide  $\text{Cl}^-$  channel: identification of a residue important in anion binding and conduction. *J Gen Physiol.* 2004;123:327-340.
- Qu Z, Hartzell HC. Determinants of anion permeation in the second transmembrane domain of the mouse bestrophin-2 chloride channel. *J Gen Physiol.* 2004;124:371-382.
- Qu Z, Chien L-T, Cui Y, Hartzell HC. The anion-selective pore of the bestrophins, a family of chloride channels associated with retinal degeneration. *J Neurosci.* 2006;26:5411-5419.
- Tsunenari T, Nathans J, Yau KW.  $\text{Ca}^{2+}$ -activated  $\text{Cl}^-$  current from human bestrophin-4 in excised membrane patches. *J Gen Physiol.* 2006;127:749-754.
- Chien L-T, Zhang Z, Hartzell HC. Single  $\text{Cl}^-$  channels activated by  $\text{Ca}^{2+}$  in drosophila S2 cells are mediated by bestrophins. *J Gen Physiol.* 2006;128:247-259.
- Yu K, Cui Y, Hartzell HC. The bestrophin mutation A243V, linked to adult-onset vitelliform macular dystrophy, impairs its chloride channel function. *Invest Ophthalmol Vis Sci.* 2006;47:4956-4961.
- Marchant D, Yu K, Bigot K, et al. New VMD2 gene mutations identified in patients affected by Best Vitelliform Macular Dystrophy. *J Med Gen.* 2007;44:e70.
- Marmorstein LY, Wu J, McLaughlin P, et al. The LP of the electroretinogram is dependent on voltage-gated calcium channels and antagonized by bestrophin (Best-1). *J Gen Physiol.* 2006;127:577-589.
- Rosenthal R, Bakall B, Kinnick T, et al. Expression of bestrophin-1, the product of the VMD2 gene, modulates voltage-dependent  $\text{Ca}^{2+}$  channels in retinal pigment epithelial cells. *FASEB J* 2006; 20:178-180.
- Lotery AJ, Munier FL, Fishman GA, et al. Allelic variation in the VMD2 gene in best disease and age-related macular degeneration. *Invest Ophthalmol Vis Sci.* 2000;41:1291-1296.
- Strauss O. The retinal pigment epithelium in visual function. *Physiol Rev.* 2005;85:845-881.
- Renner AB, Tillack H, Kraus H, et al. Late onset is common in Best macular dystrophy associated with VMD2 gene mutations. *Ophthalmology.* 2005;112:586-592.
- Mullins RF, Oh KT, Heffron E, Hameman GS, Stone EM. Late development of vitelliform lesions and flecks in a patient with Best Disease. *Arch Ophthalmol.* 2006;123:1588-1594.
- Tsien RY, Pozzan T. Measurements of cytosolic free  $\text{Ca}^{2+}$  with Quin-2. *Methods Enzymol.* 1989;172:230-262.
- Marmorstein AD, Kinnick TR. Focus on molecules: bestrophin (Best-1). *Exp Eye Res.* Published online May 23, 2006.
- Milenkovic VM, Rivera A, Horling F, Weber BHF. Insertion and topology of Normal and mutant bestrophin-1 in the endoplasmic reticulum membrane. *J Biol Chem.* 2007;282:1313-1321.

39. Seddon JM, Afshari MA, Sharma S, et al. Assessment of mutations in the Best macular dystrophy (VMD2) gene in patients with adult-onset foveomacular vitelliform dystrophy, age-related maculopathy, and bull's-eye maculopathy. *Ophthalmology*. 2001;108:2060-2067.
40. Pollack K, Kreuz FR, Pillunat LE. Best's disease with normal EOG: case report of familial macular dystrophy (in German). *Ophthalmologie*. 2005;102:891-894.
41. Wabbels B, Preising MN, Kretschmann U, Demmler A, Lorenz B. Genotype-phenotype correlation and longitudinal course in ten families with best vitelliform macular dystrophy. *Graefes Arch Clin Exp Ophthalmol*. 2006;244:1453-1466.
42. Stohr H, Marquardt A, Nanda I, Schmid M, Weber BH. Three novel human VMD2-like genes are members of the evolutionary highly conserved RFP-TM family. *Eur J Hum Gen*. 2002;10:281-284.
43. Marmorstein AD, Stanton JB, Yocom J, et al. A model of Best vitelliform macular dystrophy in rats. *Invest Ophthalmol Vis Sci*. 2004;45:3733-3739.
44. Welsh MJ, Ramsey BW, Accurso F, Cutting GR. Cystic fibrosis. In: Scriver CR, Beaudet AL, Sly WS, Valle D, eds. *The Metabolic and Molecular Bases of Inherited Disease*. McGraw-Hill, New York. 2001:5121-5188.